

Research Article

A New Method for Airborne Sound Detection Using Total Internal Reflection and Its Application to Microphone

Yasushi Suzuki¹ and Ken'iti Kido²

¹ Department of Electronic Media Technology, Gunma National College of Technology, 580 Toriba-cho, Maebashi 371-8530, Japan

² Tohoku University, 543-1-504 Niiharu-cho, Midori-ku, Yokohama 226-0017, Japan

Correspondence should be addressed to Yasushi Suzuki, suzuki@elc.gunma-ct.ac.jp

Received 2 August 2011; Accepted 24 August 2011

Academic Editor: Saulius Juodkazis

Copyright © 2011 Y. Suzuki and K. Kido. This is an open access article distributed under the Creative Commons Attribution License, which permits unrestricted use, distribution, and reproduction in any medium, provided the original work is properly cited.

A new method for detecting the sound pressure in air, which uses the total internal reflection at the curved interface between glass and air, is proposed, and its application to microphone is discussed. The critical angle for total reflection changes by the refractive index of air, which depends on the air density. The density changes by the sound pressure. Therefore, the sound pressure is measurable by detecting the intensity of the reflected light from the total reflection area. The sound pressure sensitivity of the proposed method is investigated theoretically and experimentally. Experimental results show that the microphone using the method is feasible though its sensitivity is low in the present stage. When the sensitivity is improved dramatically for practical use, the microphone becomes very sensitive to the surrounding conditions. A method to compensate the fluctuation of atmospheric pressure or temperature is presented.

1. Introduction

Ordinary microphones have a limitation in frequency range and a difficulty for the measurement of great volume of sound as the mechanical vibration is used when the sound pressure is transformed to the electrical signal. Therefore, the development of new method for electroacoustic conversion without a diaphragm has recently been expected, especially in the field of next-generation audio, impulsive noise measurement, or airborne ultrasound. Using light is an effective way to meet the requirement.

Some studies on the detection methods for airborne sound without diaphragm using optical measurement techniques have been reported [1–5]. The change in the refractive index of air due to the sound pressure is detected in those reports. However, there is no method which can measure the sound pressure at a point in the sound field with high sensitivity.

We have proposed a method, which can detect the sound pressure at a point in the sound field using the total internal reflection at a curved interface between glass and air, and demonstrated the feasibility of a microphone by use of the method theoretically and experimentally [6, 7].

The sound pressure changes the refractive index of air, which causes the change in the optical reflectance. Therefore, the sound pressure is measurable by detecting the change in the intensity of reflected light. The drawback of the ways to detect the sound pressure using the change in the optical reflectance is that the sensitivity is low because the pressure change in air due to sound is extremely small compared to the atmospheric pressure. However, the problem can be overcome by using the total internal reflection.

In this paper, besides the results of the previous report [7], a major problem caused by the fluctuation of the surrounding conditions when the microphone is put into practical use is investigated, and a solution to the issue is proposed. The gas pressure sensitivity is also verified experimentally as the microphone is essentially a pressure sensor, which indicates that the microphone can detect a large volume of sound. The maximum value of measurable sound pressure is provided.

2. Principle

Figure 1 shows the principle of the proposed method for detecting the sound pressure. When a parallel light beam is

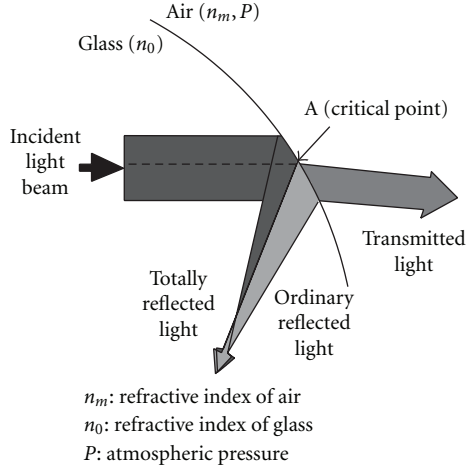


FIGURE 1: Reflection and transmission of parallel light at the interface.

incident at the curved boundary surface between glass and air, each ray of the beam has different angle of incidence. The upper ray in the beam has greater angle of incidence than the lower one. If the ray incident on the position A has the critical angle, the rays above A are totally reflected (*totally reflected light*) and some of the rays below A also reflected (*ordinary reflected light*), whereas most of them penetrate through the glass surface (*transmitted light*). The critical angle changes by the change in the refractive index of air due to sound, causing the fluctuation of position A, which produces the change in the amount of totally reflected light. Therefore, the sound pressure can be detected by measuring the intensity of reflected light.

The critical angle for total reflection θ_C is given by (1). The relation between the change in refractive index of air Δn_m and the sound pressure ΔP is expressed by (2) [6]

$$\theta_C = \sin^{-1} \frac{n_m}{n_0}, \quad (1)$$

$$\Delta n_m = \frac{n_m - 1}{\gamma P} \Delta P, \quad (2)$$

where γ is the ratio of specific heat. The sensitivity for sound pressure detection σ is defined by

$$\sigma(P) = \frac{1}{W} \frac{dS}{dP}, \quad (3)$$

where W is the total amount of incident light and S is the quantity of reflected light.

3. Calculation of the Sound Pressure Sensitivity

A sensing surface for detecting the sound pressure is made by cutting a part off from a glass rod with a radius R , as shown in Figure 2. The sensitivity of the sensor is calculated by the following procedure.

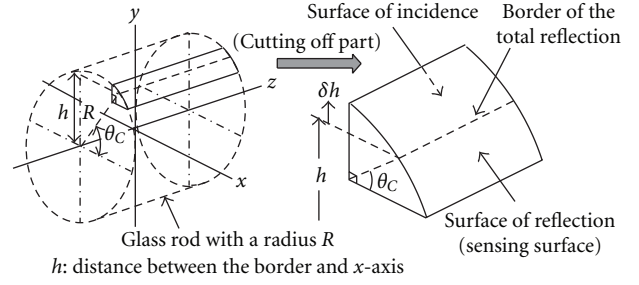


FIGURE 2: Sensing part for detecting the sound pressure.

The reflectances for p - and s -polarized light are given as follows, respectively, according to the Fresnel reflection equations for the intensity:

$$K_p = \left(\frac{n^2 \cos \theta_i - \sqrt{n^2 - \sin^2 \theta_i}}{n^2 \cos \theta_i + \sqrt{n^2 - \sin^2 \theta_i}} \right)^2, \quad (4)$$

$$K_s = \left(\frac{\cos \theta_i - \sqrt{n^2 - \sin^2 \theta_i}}{\cos \theta_i + \sqrt{n^2 - \sin^2 \theta_i}} \right)^2,$$

where θ_i is the angle of incidence and $n = n_m/n_0$. If $\theta_i \geq \theta_C$, the reflectances are not expressed by (4) and they are given as $K_p = K_s = 1$.

For simplifying the calculation, we use the approximate expressions of (4). If δh is the distance from h in the direction to y -axis in Figure 2, the relation between θ_i and the incident position δh is given by

$$\sin \theta_i = n + \frac{\delta h}{R}, \quad \cos \theta_i = \sqrt{1 - \left(n + \frac{\delta h}{R} \right)^2}, \quad (5)$$

where $\delta h \leq 0$ because $K_p = K_s = 1$ in the case that $\delta h > 0$. By substituting (5) into (4), using $|\delta h/R| \ll 1$ and $\sqrt{-\delta h/R} \ll 1$, (4) are calculated to the first-order approximations to be [7]

$$K_p \cong 1 - \frac{4\sqrt{2}}{n^2} \sqrt{\frac{n}{1-n^2}} \cdot \sqrt{-\frac{\delta h}{R}}, \quad (6)$$

$$K_s \cong 1 - 4\sqrt{2} \sqrt{\frac{n}{1-n^2}} \cdot \sqrt{-\frac{\delta h}{R}}.$$

In order to calculate the sensitivity, we use the reflectances in (6) and suppose that the incident beam shapes a rectangle and has a width of $2r_0$ as shown in Figure 3. Figure 3 illustrates that the change in the intensity of reflected light by the sound pressure. r is the distance from the surface of $y = h$. When there is no sound, the reflectance for the incident beam light is expressed by the solid line as the function of incident position. The critical point expressing the boundary line of the total reflection region is at h . If the atmospheric pressure increases by sound, the critical point moves δh to the right as shown in Figure 3. Consequently, the intensity of the reflected light decreases. When the critical

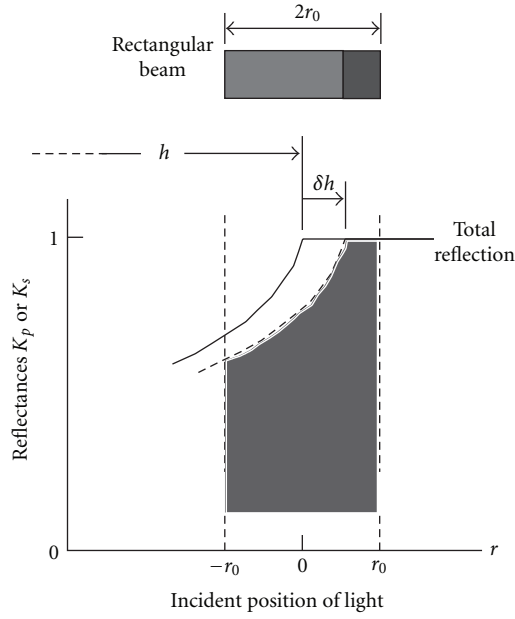


FIGURE 3: Approximated reflectance curve.

point is at $h + \delta h$ as shown in Figure 3, the intensity of p -polarized reflected light is computed as follows:

$$\begin{aligned} S_p(\delta h) &= W - \left[- \int_{-r_0-\delta h}^0 \{K_p(r) - 1\} dr \right] \\ &= 2r_0 - \frac{8\sqrt{2}}{3n^2} \sqrt{\frac{n}{1-n^2}} \cdot \frac{(r_0 + \delta h)^{3/2}}{\sqrt{R}}, \end{aligned} \quad (7)$$

where $W = 2r_0 \times 1$. The change ratio of S_p to δh at $\delta h = 0$ is calculated as follows:

$$\left. \frac{dS_p(\delta h)}{d\delta h} \right|_{\delta h=0} = -\frac{4\sqrt{2}}{n^2} \sqrt{\frac{n}{1-n^2}} \cdot \sqrt{\frac{r_0}{R}}. \quad (8)$$

The sensitivity for detecting the sound pressure is computed by using (3) as the following formula:

$$\sigma_p(P) = \frac{1}{W} \frac{dS_p}{dP} = \frac{1}{2r_0} \cdot \frac{dS_p}{d\delta h} \cdot \frac{d\delta h}{dP}. \quad (9)$$

By using (1), (2), and $\theta_C = \sin^{-1}(h/R)$ obtained in Figure 2, the next equation is given as the relation between the movement of critical point δh and the sound pressure δp [6]

$$\delta h = \frac{n_m - 1}{n_0 \gamma P} R \cdot \delta p. \quad (10)$$

The sensitivity for p -polarized light is given by using (8) and (10) as the following expression:

$$\sigma_p(P) = -\frac{2\sqrt{2}}{n^2} \sqrt{\frac{n}{1-n^2}} \cdot \frac{n_m - 1}{n_0 \gamma P} \cdot \sqrt{\frac{R}{r_0}} \quad [\text{Pa}^{-1}]. \quad (11)$$

The similar expression for s -polarized light is given by

$$\sigma_s(P) = -2\sqrt{2} \sqrt{\frac{n}{1-n^2}} \cdot \frac{n_m - 1}{n_0 \gamma P} \cdot \sqrt{\frac{R}{r_0}} \quad [\text{Pa}^{-1}]. \quad (12)$$

Since the sensitivities are proportional to $\sqrt{R/r_0}$, if we make R/r_0 larger, the sensitivities will be higher. Therefore, the microphone using the proposed method is feasible. The difference between σ_p and σ_s is only a term $1/n^2$.

4. Maximum Value of Measurable Sound Pressure

The sound pressure is detected by use of the fluctuating border of the total reflection area in the incident light beam due to sound pressure. If the border moves across the edge of the beam, the method is not available for the measurement. Therefore, when the initial position of the border is located at the center of the beam, the value of measurable sound pressure becomes a maximum. The maximum value is given by the following equation, substituting $\delta h = r_0$ into (10)

$$\delta p_{\max} = \frac{n_0 \gamma P}{n_m - 1} \cdot \frac{r_0}{R}. \quad (13)$$

A sketch of the relation between δp_{\max} and R/r_0 is shown in Figure 4, using the following values for a red light with the wavelength $\lambda = 633$ nm at the normal temperature (20°C) and the normal pressure ($P = P_0 = 1013$ hPa):

$$n_0 = 1.51633, \quad n_m(P_0) = 1.0002713, \quad \gamma = 1.403. \quad (14)$$

Figure 4 shows that the greater R/r_0 is (the greater the sensitivity is), the narrower the range of measurable sound pressure becomes.

5. Experiments

5.1. Sensitivity of the Change in Gas Pressure. The proposed sensor is essentially a pressure sensor. We verify experimentally the gas pressure sensitivity. Figure 5 shows the gas pressure sensor employed for the experiment. The sensing part made of glass with the radius of curvature of $R = 50$ cm is unified with a diode laser (LD: $\lambda = 635$ nm) and a photo diode (PD). The laser beam is linearly polarized and shapes an ellipsoid of about $1 \text{ mm} \times 3 \text{ mm}$. We adopt 1 mm as the beam width, which means that we use a s -polarized light, according to a polarimetry. The incident light on the interface is positioned by hand, measuring the relation between the scales marked on the plate supporting the sensing part and the output DC voltage from the PD circuit.

Figure 6 demonstrates the output voltage of the sensor in a container filled with nitrogen gas as the function of the gas pressure. The output voltage decreases as the gas pressure increases, which indicates that the sensor can detect the change in gas pressure, that is, a great volume of sound pressure.

The slope of the regression line in Figure 6 is about -0.095 V/atm which can be converted to the sensitivity for the change in gas pressure,

$$\eta_s(P_0) = -9.79 \times 10^{-3} \quad [\text{atm}^{-1}], \quad (15)$$

using the corresponding value of voltage, 9.7 V, to the total amount of incident light in this case. The theoretical

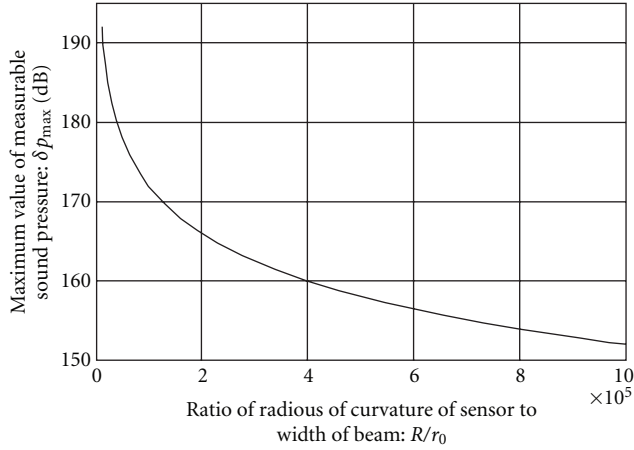


FIGURE 4: Maximum value of measurable sound pressure as the function of R/r_0 .

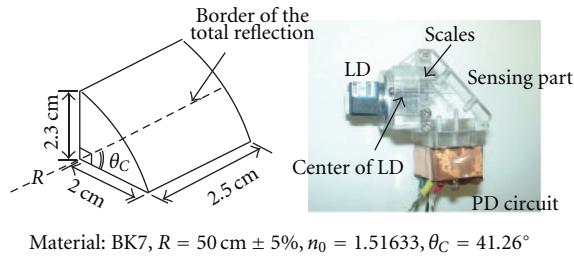


FIGURE 5: Sensing part and unified gas pressure sensor.

sensitivity can be calculated using (4) and (2) substituted $\gamma = 1$ (isothermal change) as follows:

$$\eta_s(P_0) = -17.3 \times 10^{-3} \text{ [atm}^{-1}\text{]}. \quad (16)$$

It is considered that the difference between the values in (15) and (16) is caused by the incident light beam which is not set to the optimal position (at which the border of total reflection lies down the center in the beam) in the experiment. If the incident beam can be set at the optimal position, the experimental and theoretical values will almost correspond with each other.

5.2. Verification of Work as Microphone [7]. A sensor with the radius of curvature of $R = 11 \text{ m}$ is employed for detecting the sound pressure. An LD ($\lambda = 635 \text{ nm}$) having a circular beam whose diameter is about 1 mm is used as a light source, and a PD is used for receiving the reflected light. According to (11), (12), and (14), the theoretical sound pressure sensitivities of the sensor are computed as follows:

$$\begin{aligned} \sigma_p(P_0) &= -1.31 \times 10^{-6} \\ \sigma_s(P_0) &= -0.571 \times 10^{-6} \end{aligned} \text{ [Pa}^{-1}\text{]}. \quad (17)$$

Figure 7 shows the schematic diagram of the proposed method for detecting the sound pressure arranged on an optical bench. Three types of experiment are carried out

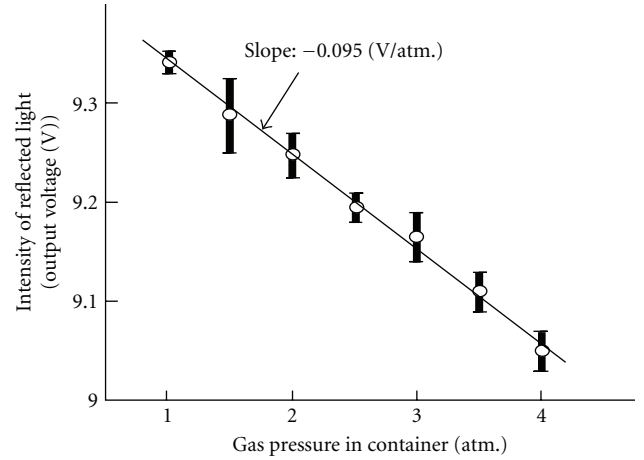


FIGURE 6: Intensity of reflected light as the function of the gas pressure in a container.

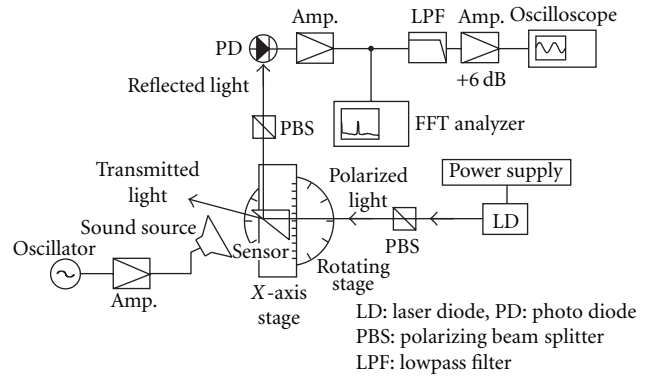
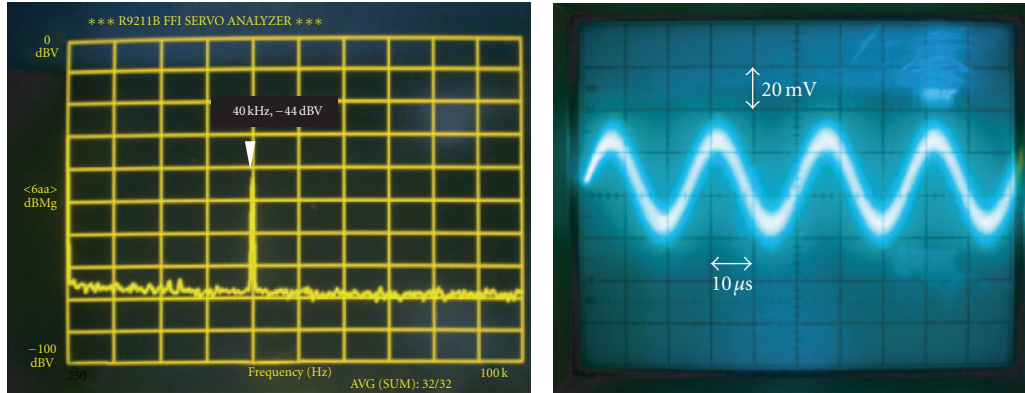


FIGURE 7: Schematic diagram of the basic configuration for sound detection.

using a different sound source in the case of each experiment. The experiments are (1) detection of sinusoidal sound wave, (2) investigation of the effect of vibration in the measurement system, and (3) detection of high pressure impulsive sound. The incident light beam is adjusted to the optimal position by using an x -axis stage and a rotating stage, referring to the power spectrum of the output signal from the PD circuit by an FFT analyzer.

5.2.1. Detection of Sinusoidal Sound Wave. Figure 8 shows the power spectra and the waveform of the output signal in the case of p -polarized light when an ultrasonic transducer with the oscillating frequency (f_0) of 40 kHz employed as sound source is set about 1.5 cm apart from the sensor. The sound pressure on the sensing surface is estimated by about 140 dB .

The outstanding peak at 40 kHz in the power spectra can be observed and the waveform can be seen clearly though S/N is low in Figure 8, which indicates that the sound pressure can be measurable by the proposed microphone. The output voltage level is about -44 dBV , whereas the value of that can be calculated to about -50 dBV using (17), because the output DC voltage of PD circuit is about 12.5 V .



Noise voltage ≈ 3.5 mV, signal voltage 13 mV; S/N ≈ 11 dB

FIGURE 8: Power spectra and waveform of the output signal (p -polarized light).

It is considered that the sound pressure at the measuring point goes up by the effect of reflected sound from the environment.

The waveforms of output signal employed two ultrasonic oscillators with 110 kHz and 200 kHz of oscillating frequencies, respectively, as sound sources are shown in Figure 9. The waveform of each high frequency sound can be detected. It can be easily expected that higher frequency sound can be measurable.

The proposed microphone has no limitation in frequency range in principle. In reality, however, the sensitivity of the microphone must be compensated since it is affected by the diffraction effect related to its size in high frequency region. If the size which does not need to compensate the sensitivity is assumed to be about 1/10 of the wavelength, the limit in frequency range is about 680 kHz when the edge of core of an optical fiber with the diameter of $50 \mu\text{m}$ can be utilized as the sensing surface.

5.2.2. Effects of Vibration of the Measurement System. Figure 10 shows the experimental arrangement around the sensor for examining the effect of vibration of the system. The laser light emitted from LD is split into two beams by a nonpolarizing beam splitter. One is incident on a region involving the border with the total reflection area as the signal light. The other is incident on the total reflection area as the reference light for monitoring the vibration of the system. Besides the ultrasonic transducer, a tweeter (Sound Pressure Level: 100 dB/W(m), 4–40 kHz) is used for the sound source and is placed about 3 cm apart from the sensor to get a high sound pressure. The input to the tweeter is 1 W, so the sound pressure level at the sensing surface is considered to be about 130 dB in this case. Each beam is received by a photodiode, and the outputs are analyzed by the FFT analyzer.

Figure 11 shows the power spectra of the signal light and the reference light in the cases that the driving frequencies of the sound sources are 40 kHz, 14.5 kHz, and 12 kHz, respectively.

Each signal light has a peak spectrum at the driving frequency in the spectra, which indicates that the microphone detects the sound pressure. The reference light in

Figure 11(c) has a peak at the driving frequency in the spectra, whereas that in Figure 11(a) or 11(b) has no peaks in its spectra. Therefore, in this case of arrangement the microphone can be affected by the vibration of the system up to the driving frequency of about 12 kHz. However, it is considered that the effect of vibration can be removed by fixing the LD and PD to the sensor.

5.2.3. Detection of an Impulsive High Pressure Sound Using p -Polarized Light. Figure 12 shows the experimental arrangement around the sensor. *Hyoshigi* is used as an impulsive sound source and is clapped about 7 cm away from the sensor. The sound level meter adjusted to have flat frequency response is placed about 60 cm apart from the sound source, monitoring the sound pressure.

The output of the PD circuit is observed by the oscilloscope passing through the LPF (70 kHz) and the amplifier (+6 dB) with the output of the sound level meter.

The observed waveforms of the outputs are shown in Figure 13. Although the S/N is low, the microphone detects the impulsive sound. Figure 13 indicates that the microphone can detect much higher frequency components than the sound level meter when the frequency range is limited under 20 kHz. The time lag of about 1.5 ms exists between the waveforms, which is caused by the separation of about 53 cm between the sensor and the sound level meter.

The waveform (a) predicts the maximum sound pressure of about 140 dB at the sensing surface because its peak value is about 130 dB. From the waveform (b), however, the peak of the sound pressure at the sensing surface is estimated to be about 164 dB, using (17) and the measured values that are 100 mV (the peak value of the waveform) and 12.5 V (the output DC voltage of the PD circuit).

6. Effects of the Fluctuation of Surrounding Conditions

The refractive index of air changes by the fluctuation of the surrounding conditions such as atmospheric pressure and temperature. The refractive index of air for the red light of He-Ne laser around the industrial normal state

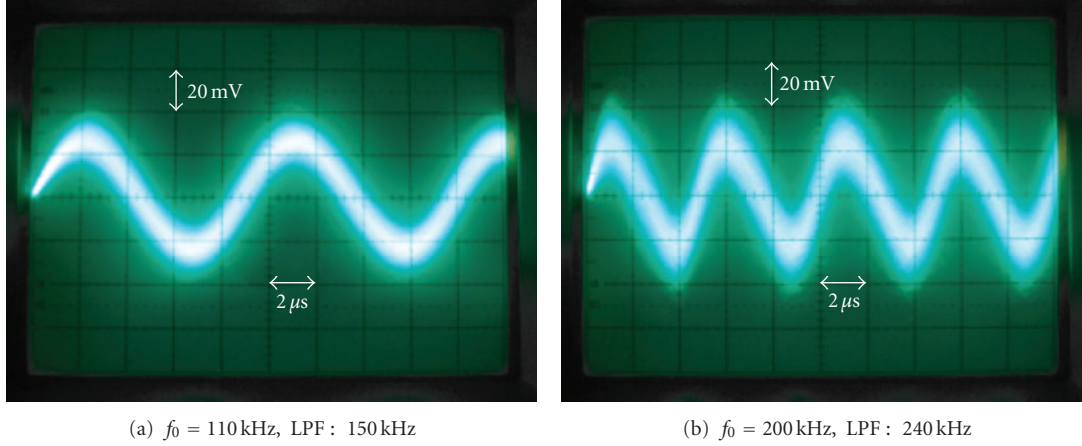


FIGURE 9: Waveforms of the output signal (p -polarized light).

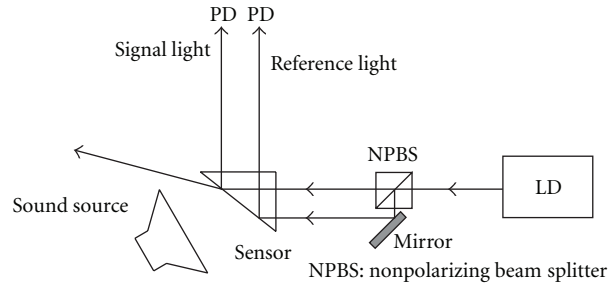


FIGURE 10: Experimental arrangement around the sensor for examining the effect of vibration.

(temperature: 20°C , atmospheric pressure: 1013 hPa, vapor pressure: 13.33 hPa, and concentration of CO_2 : 0.03%) is approximately given by the following equation [8]:

$$\begin{aligned}
 (n_m - 1) \times 10^6 &= 271.30 - 0.93(T - 20) \\
 &+ 0.27(P - 1013) - 0.0375(P_w - 13.33) \\
 &+ 0.02(k - 3),
 \end{aligned} \tag{18}$$

where T is a temperature in $^\circ\text{C}$, P and P_w are the atmospheric pressure and the vapor pressure in hPa, respectively, and k is the concentration of the carbon dioxide in 0.01% unit.

The atmospheric pressure and the temperature affect the refractive index of air much more largely than the other conditions do. The biggest problem caused by the fluctuation of surrounding conditions is that the critical point can move outside the incident beam. The proposed microphone will lose the sensitivity in such the case. It is significant when the radius of curvature of the curved surface is made very large to improve the sensitivity for detecting an ordinary magnitude of sound as well as a large volume of sound. In this section, we investigate the influence of the fluctuation of atmospheric pressure and temperature and present a way to resolve the problem.

6.1. Measurable Range of Sound Pressure. Figure 14 shows how the measurable range of sound pressure is reduced

by the movement of the border due to the fluctuation of surrounding conditions.

The maximum value of measurable sound pressure considering the fluctuation of atmospheric pressure and temperature is expressed by using (13) and (18) as follows:

$$\begin{aligned}
 \delta p_{\max} &= \frac{n_0 \gamma P_0}{n_m - 1} \frac{r_0}{R} \\
 &\times \left\{ 1 - \frac{R}{r_0} \frac{|-0.93(T - 20) + 0.27(P - 1013)|}{n_0} \times 10^{-6} \right\}.
 \end{aligned} \tag{19}$$

The border of the total reflection is expressed by $h = (n_m/n_0)R$. Let Δn_m be the fluctuation of the refractive index of air, then the permitted range Δh is given by

$$\Delta h = \frac{\Delta n_m}{n_0} R \leq |r_0|. \tag{20}$$

Therefore, the allowable range of the atmospheric pressure P [hPa] can be computed as the function of temperature and r_0/R :

$$\begin{aligned}
 &\left\{ 3.44(T - 20) - 5.62 \left(\frac{r_0}{R} \times 10^6 \right) \right\} + 1013 \\
 &\leq P \leq \left\{ 3.44(T - 20) + 5.62 \left(\frac{r_0}{R} \times 10^6 \right) \right\} + 1013.
 \end{aligned} \tag{21}$$

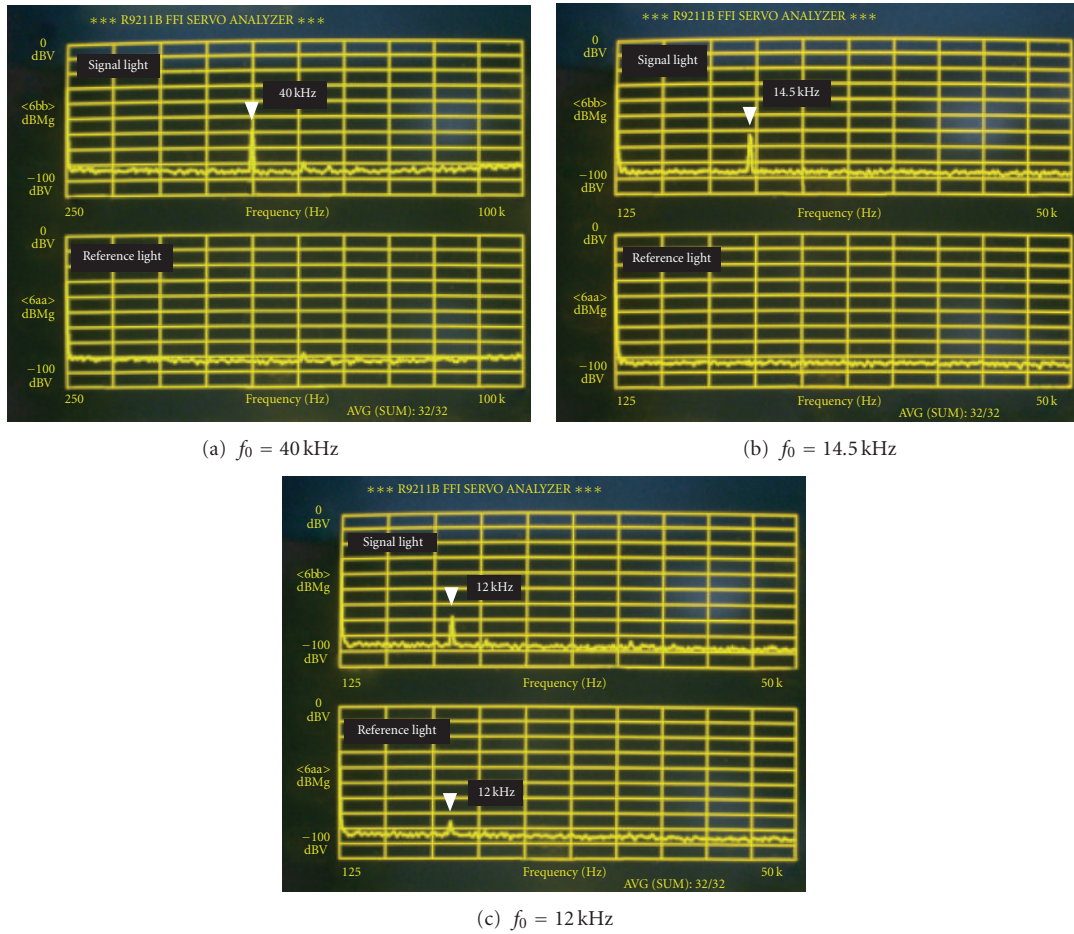


FIGURE 11: Power spectra of the signal light (top) and the reference light (bottom).

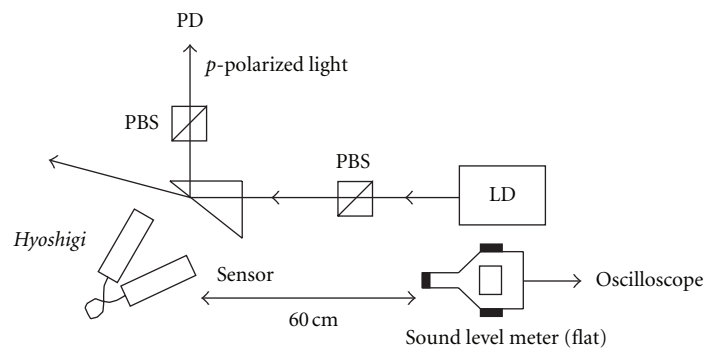


FIGURE 12: Experimental arrangement around the sensor for detecting an impulsive high pressure sound.

The allowable range of the atmospheric pressure computed by (21) is plotted in Figure 15. The area shut in by a pair of lines is the range for the microphone to have the sensitivity. If R/r_0 is increased to get higher sensitivity, the range becomes narrower. Therefore, it is needed for practical use with the invention to adjust the sensing part automatically and conform the incident angle of the beam to the critical angle, according to the movement of the border of the total reflection due to the fluctuation of the surrounding conditions.

6.2. Automatic Adjustment of the Angle of Incidence Using Two Incident Beams. The reduction of the range of sound pressure detection caused by the fluctuation of surrounding conditions can be prevented by resetting the border of the total reflection to the initial position, detecting the movement of the border. Figure 16 indicates a method for adjusting automatically the angle of incidence of the light beams.

The p -polarized signal light and the s -polarized reference light from an LD are located very close and propagate

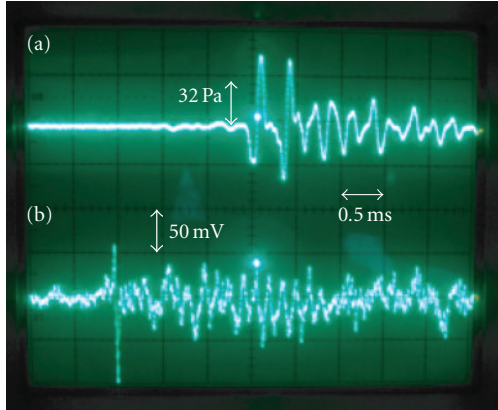


FIGURE 13: Waveforms of the output signal of the sound level meter (a) and the proposed microphone (b).

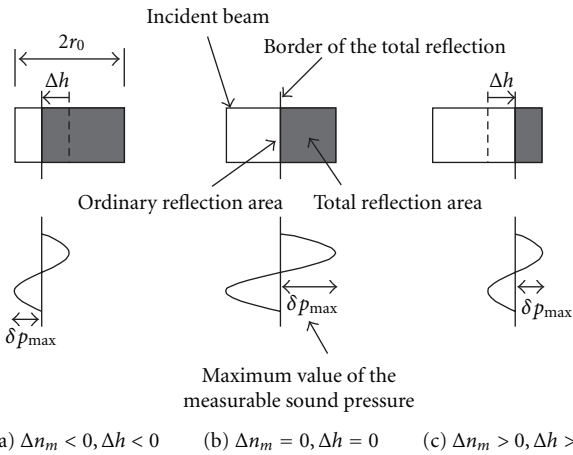


FIGURE 14: Reduction of the measurable range of sound pressure due to the fluctuation of surrounding conditions.

parallel to each other. The distance between the two (d) is extremely small. The two beams can be slightly deflected by a deflector to make the difference between the intensities of the two beams reflected from the sensing surface zero by controlling the driving voltage of the deflector, according to the movement of the border due to the fluctuation of surrounding conditions. d is the distance of which the reflectances of p - and s -polarizations are equal to each other. The incident angle of the ray in the center of the signal light beam can be always kept to the critical angle by using the deflector. The experimental investigation about the adjusting method is a future work.

7. Conclusion

This paper describes a new method for measuring the airborne sound at one point in a sound field which uses the total internal reflection on a curved interface between glass and air and discusses its application to microphone without mechanical vibration theoretically and experimentally. The validity of the proposed method is verified by calculation,

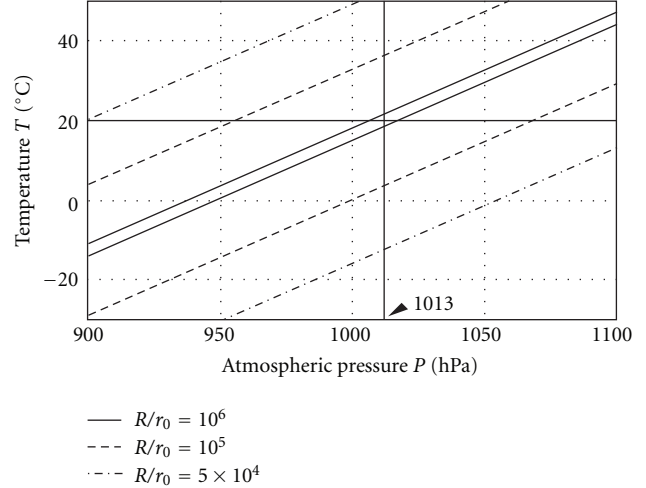


FIGURE 15: Range of the surrounding conditions for the microphone to have the sensitivity.

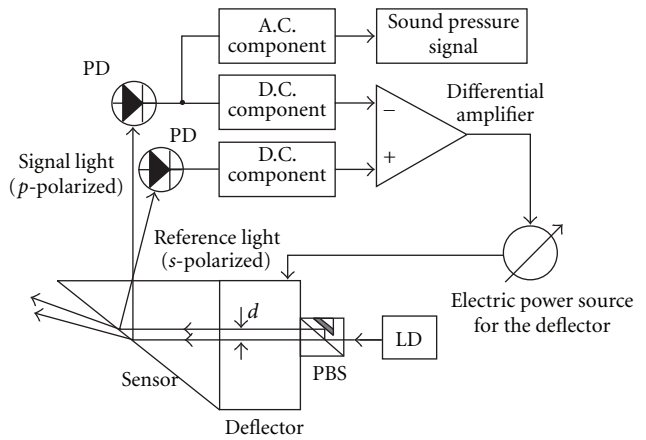


FIGURE 16: Principle of automatic adjustment of incident angle using two beams and a deflector.

and the feasibility of the microphone using the method is experimentally clarified. The experimental results show that the proposed microphone can be used for detecting an extremely high frequency and a great volume of sound.

In order to detect the waveform of ordinary pressure sound, the sensitivity of the microphone is needed to be improved by making the radius of curvature of the sensing surface R large, but the sensor with very large R is extremely sensitive to the fluctuation of the surrounding conditions. It is shown that the problem can be overcome by controlling the direction of the incident beam automatically using a deflector, although the highly advanced optical techniques would be required. The experimental investigation of the control method will be carried out in the next stage.

The proposed method will make microminiaturized and wide-ranged microphone possible to be in practical use.

Acknowledgment

This work was supported in part by a Grant-in-Aid for Scientific Research (C) (22560434) from Japan Society for the Promotion of Science.

References

- [1] K. Nakamura, M. Hirayama, and S. Ueha, "Visualization of sound pressure distributions by optical detection of the modulation in the reflective index of air," IEICE Technical Report AI2001-2-1/AA2001-23, 2001 (Japanese).
- [2] N. Saito and Y. Yamasaki, "Sound recording without diaphragm," in *Proceedings of the Autumn Meeting of the Acoustical Society of Japan*, pp. 479–480, 2002 (Japanese).
- [3] M. Iwamoto and P. K. Choi, "Measurement of airborne ultrasonic fields using optical beam deflection," *The IEICE Transactions on Electronics*, vol. J86-C, no. 12, pp. 1318–1323, 2003 (Japanese).
- [4] M. Sonoda, "Investigation of optical system for direct detection of audio-wave by optical Fourier transform," *The Journal of the Acoustical Society of Japan*, vol. 62, no. 8, pp. 571–579, 2006 (Japanese).
- [5] H. Takei, T. Hasegawa, K. Nakamura, and S. Ueha, "Measurement of intense ultrasound field in air using fiber optic probe," *Japanese Journal of Applied Physics*, vol. 46, no. 7, pp. 4555–4557, 2007.
- [6] Y. Suzuki and K. Kido, "Theoretical investigation on the sensitivity of a microphone using the change in the total reflection of light by sound," *Acoustical Science and Technology*, vol. 29, no. 4, pp. 283–290, 2008.
- [7] Y. Suzuki and K. Kido, "Experimental investigation on a microphone using the change in the total reflection of light by sound," *Acoustical Science and Technology*, vol. 30, no. 5, pp. 355–362, 2009.
- [8] Y. Sakurai, "Laser-applied measurement," *Journal of the Japan Society of Mechanical Engineers*, vol. 74, no. 624, pp. 82–89, 1971 (Japanese).



Hindawi

Submit your manuscripts at
<http://www.hindawi.com>

